Characterization of Polyorganosiloxane Nanoparticles in Aqueous Dispersion by Asymmetrical Flow Field-Flow Fractionation

Nadja Jungmann, Manfred Schmidt, and Michael Maskos*

Universität Mainz, Institut für Physikalische Chemie, Jakob-Welder-Weg 11, D-55099 Mainz, Germany

Received April 17, 2001; Revised Manuscript Received July 31, 2001

ABSTRACT: The advantages of asymmetrical flow field-flow fractionation (AF-FFF) for the characterization of aqueous dispersions of spherical polyorganosiloxane nanoparticles are discussed. With AF-FFF it was possible to obtain information about the synthesis, which is based on the hydrolysis and condensation of alkylalkoxysilanes in aqueous dispersion, and the average size of the spherical nanoparticles in the complex mixture in the presence of excess surfactant. The results are compared to measurements performed with dynamic light scattering (DLS). The size of the nanoparticles increases as a function of the amount of added monomer. Particles with radii between 2 and 50 nm are observed. If only the cross-linking monomer methyltrimethoxysilane (T) or a fixed monomer mixture of T and the chain-forming monomer diethoxydimethylsilane (D) is used, the increase in the radius shows a cube dependence on the volume of added monomer as expected. With AF-FFF it is also possible to obtain information on the role of the surfactant, which is needed to stabilize the particles. For spherical nanoparticles that are composed only of the trifunctional T or of a monomer mixture of T and D, it was found that the amount of surfactant needed to stabilize the growing particles is proportional to their surface. In the case of a more complex spherical core−shell architecture it was possible by AF-FFF analysis to obtain information about a secondary nucleation which may take place during the synthesis.

Introduction

The characterization of polymers and colloids in solution is sometimes a great challenge, especially in solutions of complex composition. For example, Mächtle et al. reported the characterization of PBA particles with grafted SAN by analytical ultracentrifugation[1] with high experimental effort. Other commonly used techniques such as static and dynamic light scattering often require additional separation of complex sample mixtures or fractionation of very polydisperse samples prior to the analysis in order to obtain useful information.[2]

AF-FFF, on the other hand, is a known and approved technique for the separation of even complex mixtures.[3] However, it is often difficult to obtain detailed information about the structural properties of the sample.[4] The advantage of AF-FFF lies in the fact that the components of a complex mixture are separated and easily characterized accordingly. This becomes possible, if the particles to be characterized can be separated from the rest of the complex mixture by AF-FFF, and in that case, AF-FFF proves to be a powerful tool in the determination of particle properties not—or at least not as easily—accessible by other techniques. This is shown with the determination of the size of organosilica nanoparticles in aqueous dispersion in the presence of surfactant. The synthesis of these spherical colloids is based on the sol−gel process, which involves the hydrolysis and condensation of alkoxysilanes in aqueous dispersion.[5−8] In comparison to the method described by Stöber et al., modified by van Blaaderen[9,10] based on tetraethoxysilane (TEOS), alkylalkoxysilanes are used for the synthesis of colloidal particles, stabilized by a surfactant. In this work methyltrimethoxysilane (T) as network-forming monomer and diethoxydimethylsilane (D) as chain-forming monomer are used in the presence of the surfactant benzethonium chloride to synthesize the polyorganosiloxane nanoparticles. Employing mixtures of T and D, it is possible to gain control over the elasticity[11] and the pore size of the resulting nanospheres.[12] The monomers or monomer mixtures are added drop- and/or stepwise, depending on the desired architecture. The first step of the synthesis is the base-catalyzed hydrolysis and condensation of the monomers in aqueous solution, followed by saturation of reactive groups at the surface of the grown particles in order to prevent irreversible aggregation and to prevail single particle properties. The nanoparticles are subsequently transferred into organic solvents and after additional surface saturation, precipitation, and isolation, they are molecularly redispersable.[5−8] A schematic overview of the complete process is given in Figure 1.

The mechanism of the formation and growth of the particles in aqueous dispersion is not yet fully understood. The small size of the particles ($2 \lesssim R \lesssim 50$ nm) and the complexity of the synthesis due to the presence and influence of the surfactant, the different monomers, and the intermediate reaction products prohibit a detailed characterization. To gain insight into this complex process, the growing particles are characterized with asymmetrical flow field-flow fractionation (AF-FFF). Employing self-made narrow spherical polyorganosiloxane standards and polystyrene microgels characterized by dynamic light scattering (DLS), the AF-FFF instrument is calibrated. The determined diffusion coefficients are then translated by the Stokes−Einstein equation into the appropriate hydrodynamic radii.

Thus, the purpose of this paper is (i) to show the advantage of the characterization of the size of spherical polyorganosiloxane nanoparticles by asymmetrical flow field-flow fractionation (AF-FFF) and (ii) to obtain detailed information about the polycondensation reaction in aqueous dispersion. The results are compared with dynamic light scattering (DLS) measurements.

Experimental Section

Materials. Water was purified with a Milli-Q deionizing system (Waters, Eschborn, Germany). Methyltrimethoxysilane

10.1021/ma0106752 CCC: $20.00
Published on Web 10/12/2001

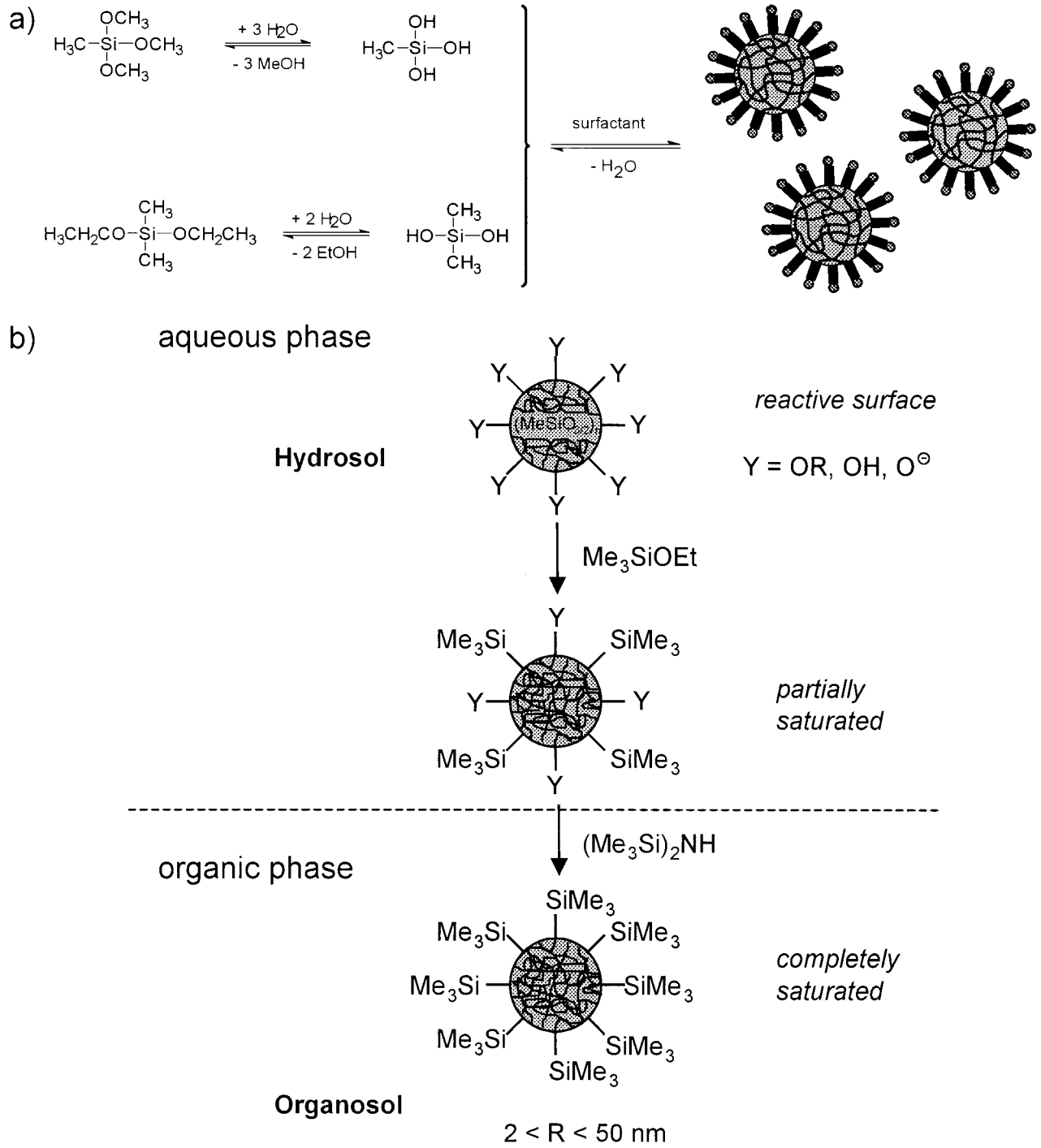

Figure 1. Schematic representation of the synthesis of spherical polyorganosiloxane nanoparticles: (a) hydrolysis of T and D and subsequent condensation in the presence of surfactant; (b) transfer from the aqueous dispersion (neglecting the surfactant) into an organic solvent (surfactant removed), which results in the formation of molecularly redispersable nanoparticles.

(T), diethoxydimethylsilane (D), and ethoxytrimethylsilane were used as received (Wacker Chemie GmbH, Burghausen, Germany). Sodium hydroxide and sodium azide (Fluka, Deisenheim, Germany), and benzethonium chloride ([2[2(*p*-1,1-3,3-tetramethylbutylphenoxy)ethoxy]ethyl]ammonium chloride) (Aldrich, Deisenheim, Germany) were used in p.a. grade as received. TWEEN 20 (Fluka) was used without further purification.

Methods. Dynamic light scattering was performed with an argon ion laser (Stabilite 2060, $\lambda = 514$ nm, Spectra-Physics, Darmstadt, Germany), a SP-125 goniometer, and an ALV-5000 multiple-τ digital correlator (ALV, Langen, Germany) at 20 °C and angles between 50° and 130° in steps of 20°. All solutions were filtered with Millex-GS filters (0.22 μm, Millipore, Eschborn, Germany). The correlation functions were analyzed by a cumulant fit or by a biexponential fit based on the simplex algorithm to determine the angular dependent diffusion coefficient D_q. The extrapolation to zero scattering angle yields the apparent diffusion coefficient D which can be translated into the appropriate hydrodynamic radius via the Stokes−Einstein relation.[13] The samples show no pronounced concentration dependence in dilute solution. For pure surfactant solutions and for solutions at the beginning of the monomer addition, two relaxation processes were observed. In these cases, the modes were separated, and the faster one was attributed to the spherical nanoparticles and the slower to larger aggregates of free surfactant (see below).

AF-FFF measurements were obtained using an AF-FFF system from Consenxus, Ober-Hilbersheim, Germany, equipped with an AF-FFF channel with PMMA cover plate, a 190 μm

Table 1. Reaction Parameters *S* (Fleet Ration), *D* (Amount of Chain-Forming Monomer), and *T* (Amount of Cross-Linking Monomer) for Different Polycondensation Procedures

sample	NaOH (10%) [mg]	surfactant [g]	*S*	*D* [g]	*T* [g]
$T_{1.5}$	300	1.5	0.06		25
$T_{2.5}$	300	2.5	0.10		25
$DT30/70_{2.5}$	300	2.5	0.10	7.5	17.5
$DT50/50_{2.5}$	300	2.5	0.10	12.5	12.5
D-$DT30/70_{3.0}$[a]	600	3.0	0.12	8/5.1	−/11.9

[a] Core composed of D, shell of D and T, respectively.

Mylar spacer, a Thermoseparations TSP constametric 3200 flow pump running at 3 mL/min, a Knauer WellChrom Micro-Star K-100 injection pump operating at 0.1 mL/min, a Bronkhorst Hi-Tec Liqui-Flow delivering a cross-flow of 2 mL/min, a degasser ERC-3114, valve box, and controller. A Waters 486-UV detector operating at 254 nm monitored the eluting particle concentrations. Regenerated cellulose membranes were utilized as semipermeable walls (MWCO 10 000 g/mol, Consenxus). Degassed Milli-Q water with NaN_3 (200 mg/L) and TWEEN 20 (100 mg/L) was used as eluent ($\eta = 0.94$ cP).[14]

Synthesis (reaction parameters are given in Table 1). If only T was used, the sample code T_x denotes the amount of surfactant as suffix *x*. In the case of mixtures of D and T, the sample code is DTx/y_z with *x* and *y* the amount of D and T (w/w), respectively, and *z* the amount of surfactant. For the core−shell spheres D-DTx/y_z was used, indicating that the core consists only of D and the shell again of a mixture of D and T.

$T_{1.5}$/$T_{2.5}$: To 125 g of Milli-Q water, 300 mg of a 10% aqueous solution (w/w) of sodium hydroxide (0.75 mmol) and 1.5 g ($S = 0.06$) for $T_{1.5}$ or 2.5 g ($S = 0.1$) for $T_{2.5}$ of benzethonium chloride were added and mechanically stirred, where *S* is the fleet ratio defined as $S = m_S/m_{mon}$ (m_S = mass of surfactant, m_{mon} = total mass of monomer). Methyltrimethoxysilane (T) (25 g, 0.18 mol) was added under continuous stirring drop- and stepwise via a syringe pump (drop rate: 25 mL/h). First, 1 g of monomer was added, and after 1 h a small amount of the sample was collected. This step was repeated four times until a total amount of 5 g of monomer was added. The next samples were drawn after addition of 5 g of monomer and 2 h reaction time each until a total of 25 g of monomer was consumed.

$DT30/70_{2.5}$, $DT50/50_{2.5}$: The method of preparation for $DT30/70_{2.5}$ was the same as for $T_{2.5}$ with 125 g of Milli-Q water, 300 mg of 10 wt % NaOH (0.75 mmol), and 2.5 g of benzethonium chloride ($S = 0.1$). The monomer mixture consisting of 7.5 g (50 mmol) of diethoxydimethylsilane (D) and 17.5 g (130 mmol) of methyltrimethoxysilane (T) was added in steps of 2, 1, and 2 g to yield 5 g of added monomer and then again in steps of 5 g to result in 25 g of total added monomer. The procedure for $DT50/50_{2.5}$ was the same, but a mixture of 12.5 g (80 mmol) of D and 12.5 g (100 mmol) of T was used.

D-$DT30/70_{3.0}$: Basically the same recipe was used for D-$DT30/70_{3.0}$ beginning with 125 g of Milli-Q water, 600 mg of 10 wt % NaOH (1.5 mmol), 3.0 g of benzethonium chloride ($S = 0.12$), and 8 g (54 mmol) of D were added within 1 h and reacted overnight. The reactive end groups of the poly(dimethylsiloxane) chains were saturated two times with 100 mg (total 1.92 mmol) of ethoxytrimethylsilane with a delay of 8 h. After stirring overnight, a total amount of 5.1 g (34 mmol) of D and 11.9 g (87 mmol) of T were added in three steps of 5 g and the last of 2 g (drop rate 18 mL/h) and delay of 2 h.

All samples were diluted with the eluent before they were measured in the AF-FFF.

Results

To prove that the results of the complex mixtures obtained with the asymmetrical flow field-flow fractionation (AF-FFF) in aqueous solution can be interpreted quantitatively, some experiments concerning the conversion of the measured retention times into hydrodynamic radii and the concentration dependence of the detector response are discussed to check the reliability of the separation observed by AF-FFF. First the instrument was calibrated with narrow spherical standards. The relation between the hydrodynamic radius R_h of the samples determined by DLS and the retention time t_R were measured by AF-FFF for a fixed quotient of cross-flow and channel outlet flow in all experiments. The data characterizing the samples are given in Table 2.

Table 2. Characterization of the Spherical Particles Used for the Calibration of the AF-FFF[a]

sample	R_h/nm	μ_2	sample	R_h/nm	μ_2
ST27	8.3	0.015	ADS367	66.5	0.02
V22	20.8	0.03	ADS284	90.0	0.02
V21	31.7	0.03			

[a] R_h and μ_2 were obtained by DLS in aqueous solution applying a cumulant fit and extrapolation to zero scattering angle and zero concentration. ST27, V22, and V21 are polyorganosiloxane particles; ADS367 and ADS284 are polystyrene latices.

From theoretical considerations it follows that the retention time t_R is related to the diffusion coefficient through[14−17]

$$t_R = \frac{w^2 \dot{V}_c}{6D\dot{V}}, \tag{1}$$

with *w* the channel height, $\dot{V}_c$ the cross-flow, $\dot{V}$ the channel outlet flow, and *D* the diffusion coefficient.

Via the Stokes−Einstein equation the diffusion coefficient is linked to the hydrodynamic radius R_h:

$$R_h = \frac{k_B T}{6\pi\eta D} \tag{2}$$

with $k_B T$ the thermal energy and η the solvent viscosity. The combination of eqs 1 and 2 yields a linear relationship between R_h and t_R:

$$R_h = \frac{k_B T \dot{V}}{\pi\eta w^2 \dot{V}_c} t_R \tag{3}$$

which would in principle allow the direct and absolute determination of the hydrodynamic radius. But since the utilized cellulose membrane may become deformed during the assembly of the channel, the channel height *w* is smaller as compared to the spacer thickness. Experiments in our lab revealed that the determination of the effective channel height w_{eff} was not reliable and precise enough utilizing only one standard. Therefore, the above-mentioned narrow spherical standards were employed to verify the linear relationship between 8 and 90 nm; i.e., the retention times determined from AF-FFF can be directly translated with the help of the linear calibration function into the corresponding hydrodynamic radii. Also, the effective channel height was determined to be $w_{eff} = 102.8$ μm, compared to the spacer thickness of 190 μm.

It is important to ensure that the results obtained with AF-FFF are not affected by overloading effects, commonly known in flow FFF, which results in a shift of the peak and partial reversible adhesion of particles on the accumulation wall.[17] Therefore, different concentrations of a dispersion (sample ST 27, Table 2) diluted with the eluent employed for AF-FFF ranging between 0.05 and 0.50% (w/w, polymer content with

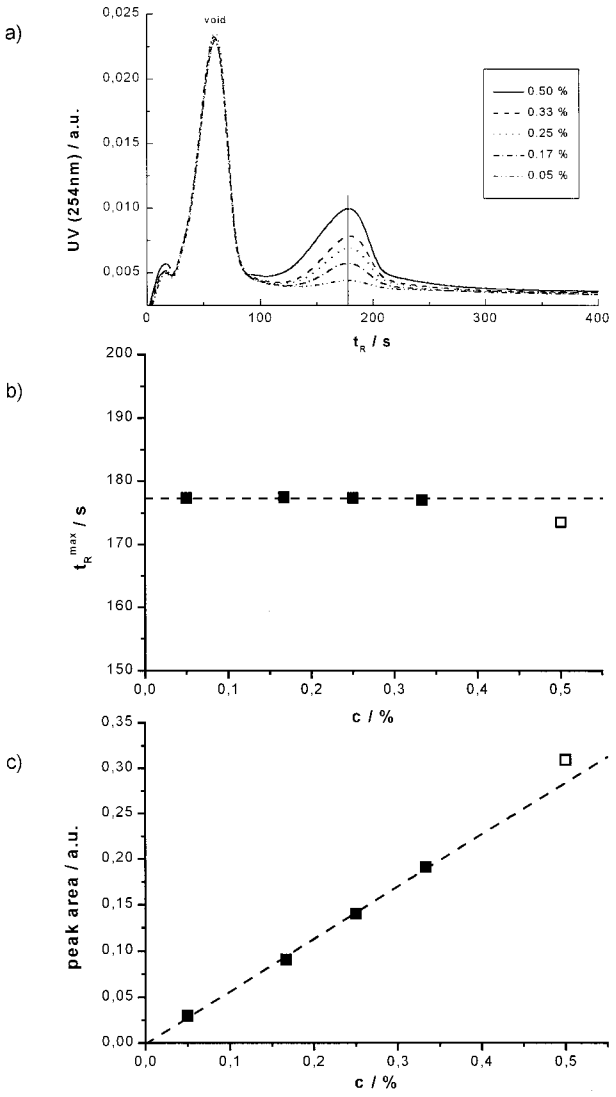

Figure 2. (a) Concentration dependence of the UV signal at 254 nm for ST27. The first peak indicates the void or system peak. Concentrations (w/w) with respect to 100% conversion. (b) Retention times of the sample peak maximum against weight concentration of ST27. The open square indicates significant deviation from the ideal behavior (concentration in w/w). (c) Peak area of the sample peaks obtained by integration, against weight concentration of ST27. The open square indicates significant deviation from the ideal behavior (concentration in w/w).

respect to 100% conversion) are separated with AF-FFF. The fractograms are given in Figure 2.

The first peak, which is virtually unaffected by the concentration of the sample, is attributed to the void or system peak. It is also present if no sample is injected into the channel. The vertical bar indicates that the position of the peak maximum does not change significantly. After linear baseline subtraction, the peak maximum is determined, giving the retention time of the sample, which is then translated into the hydrodynamic radius. The determined width of the peak is difficult to interpret quantitatively, since the instrumental band broadening[18] is in practice difficult to determine and is therefore neglected in this discussion. The maxima of the peaks of different concentrations show essentially no deviations (Figure 2b).

Only the highest concentration presented (0.50%) tends to deviate to shorter retention times and higher

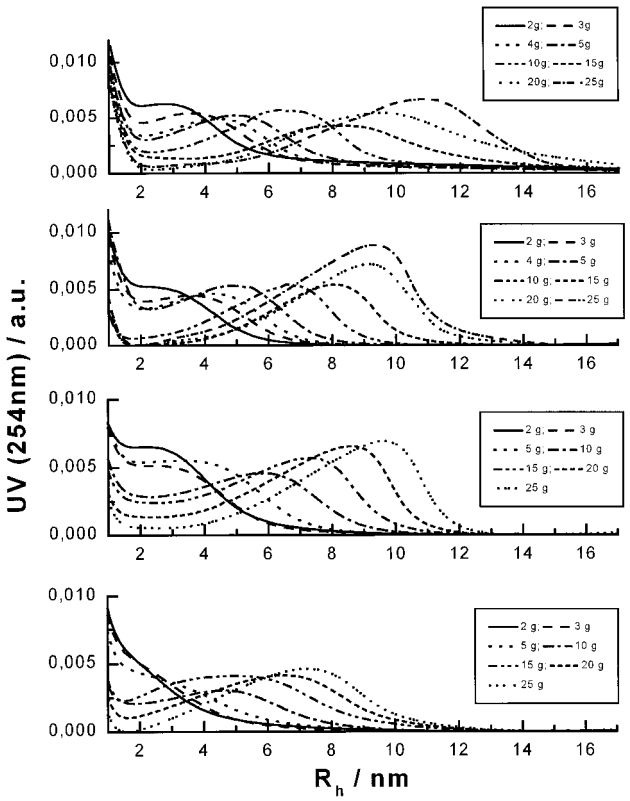

Figure 3. UV signal (254 nm) of the sample sets $T_{1.5}$, $T_{2.5}$, $DT30/70_{2.5}$, and $DT50/50_{2.5}$ (from top to bottom) obtained after addition of different amounts of monomer, as indicated by the total amount of monomer after each addition. The samples 2−5 g were diluted with eluent 1:10 (v/v), and the samples 10−25 g with eluent 1:20 (v/v). The calibration was used to translate the retention time into the corresponding hydrodynamic radius R_h.

peak area, which was determined by integration (Figure 2c). Therefore, all samples examined were kept below this concentration, in which case no sample overloading was observed. The peak area determined with the UV detector at a wavelength of 254 nm as a function of concentration shows a linear dependence, again with the exception of the highest concentration. It should be mentioned that only the surfactant is detected, since the simple siloxane monomers used in this study do not contribute significantly to the UV signal. With these basic results, the size growth of the particles in aqueous dispersion can be monitored with AF-FFF.

Homogeneous T-Nanospheres. After addition of different amounts of monomer samples are taken, diluted with the AF-FFF eluent, and injected into the instrument. The reaction parameters are given in Table 1. The fractograms are presented in Figure 3.

The figure shows only the portion of the fractograms attributed to the sample, neglecting the void peak. The *radii* corresponding to the peak maxima correlate with the amount of added monomer. This correlation yields a linear relationship between the cube of the hydrodynamic radius R_h and the added monomer volume V_T, as expected for spheres with homogeneous density. The first values have been neglected in the extrapolation, since a reasonable separation from the void peak was not possible (Figure 4).

The volume V_i (see arrows in Figure 4, denoting the possibility of the separation from the void peak in AF-FFF) is thought to be the induction volume needed to effectively promote particle growth. V_i increases from

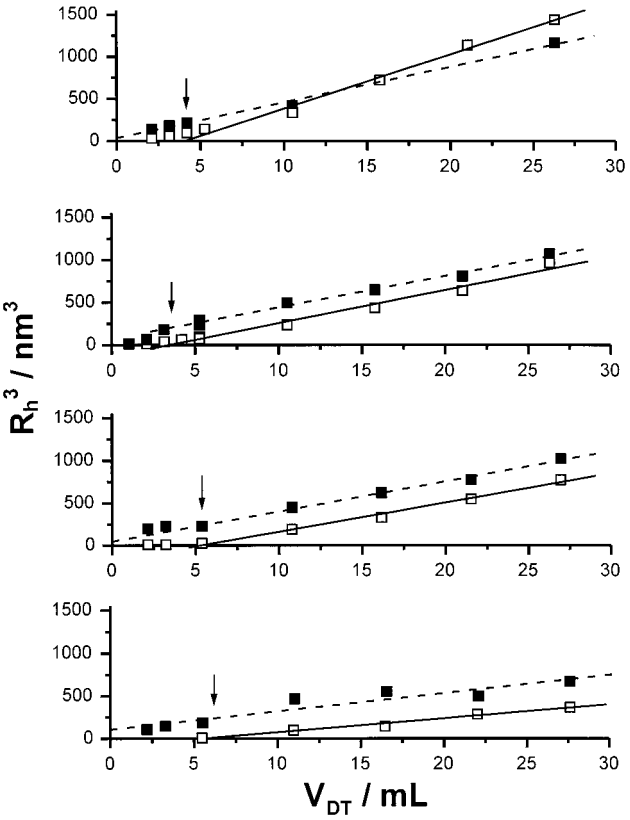

Figure 4. Comparison of the cubic mean particle hydrodynamic radius obtained by AF-FFF (open squares) and DLS (filled squares) for $T_{1.5}$, $T_{2.5}$, DT30/70$_{2.5}$, and DT50/50$_{2.5}$ (from top to bottom), plotted against the added monomer volume. The arrows mark the individual "induction" volumes V_i.

about 3.6 mL for $T_{2.5}$, to 4.1 mL for $T_{1.5}$, to 5.4 mL for DT30/70$_{2.5}$, and to 5.8 mL for DT50/50$_{2.5}$. It might also be speculated that a minimum volume of monomer is present in the solution and is not incorporated into the particles, resulting in the value for V_i. This fraction of the mixture smaller than approximately 2 nm is thought to reflect the equilibrium concentration of the monomer or very small oligomers, which might also depend on the parameters like concentration of surfactant, speed of stirring, drop rate, etc., which has to be studied in the future.

The shift between the light scattering and AF-FFF data seen in Figure 4 might be explained by the influence of polydispersity with respect to the different averages of the hydrodynamic radius accessible by DLS or AF-FFF. The effect of polydispersity is going to be investigated in the future. Since free surfactant is still present in solution, it may influence the scattering signal. The concentration of free surfactant, which is not used to stabilize the growing particles, ranges from 12 to 24 g/L, depending on the sample. The critical micelle concentration (cmc) for benzethonium chloride in aqueous solution has been studied by for example Paradies et al.[19,20] and Emmerich.[21] When neither salt nor buffer is added, the experimental value of the cmc varies between 0.9 and 1.5 g/L, depending on the method applied. When salt and buffer are added, the cmc decreases. Paradies et al. studied the formation of micelles in buffer solution and observed only small micelles with a radius of 2.55 nm. Baumann reported in addition to the micelles the presence of larger aggregates with radii of approximately 200 nm in the

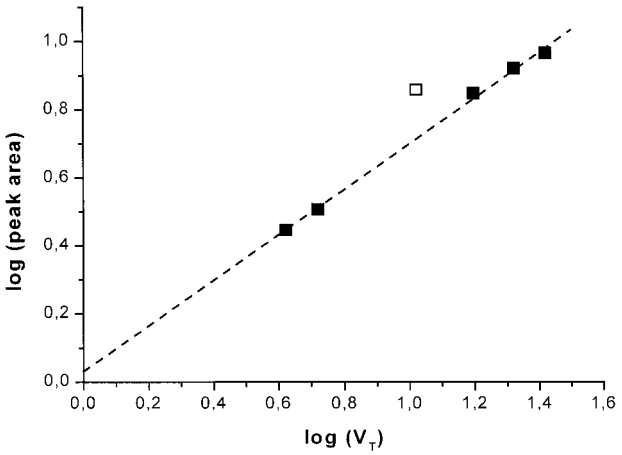

Figure 5. Double-logarithmic plot of the sample peak area in AF-FFF against the added monomer volume for $T_{1.5}$. Peak areas were determined by integration of the peak (UV signal against t_R), wherever separation from the void peak was possible. The value for V_T = 10.5 mL has been neglected for the extrapolation.

reaction mixture.[22] These micellar structures do substantially effect the light scattering signal. The relative influence is greater in the case of the smaller polyorganosiloxane nanoparticles, since upon increase of the monomer content, the amount of free surfactant decreases. AF-FFF, on the other hand, separates the excess surfactant from the nanoparticles by washing through the membrane (MWCO 10 kDa) and should therefore yield more accurate data for the nanoparticles.

An exception from the trend that the radius determined by DLS is always larger than the radius found in AF-FFF is observed for $T_{1.5}$. This sample is already at the experimental edge of stability, in which case we observe a fractionation of partly aggregated particles upon diluting and filtering prior to the DLS experiment. This is not observed in AF-FFF, because the experiments are performed immediately after obtaining the aliquot, whereas for DLS the samples have to be filtered and fractionation may occur with the $T_{1.5}$ samples. An interpretation for the different slopes observed in the size-dependent measurements for the different samples is presented below.

The response of the UV detector shows a linear dependence on the concentration of the surfactant in the eluent. As discussed above, UV detection is only sensitive to the surfactant. Since only the part of the surfactant associated with the polyorganosiloxane nanoparticles is detected, because the free surfactant is washed through the membrane and does not pass the detector, this can be used to analyze the amount of surfactant needed to stabilize the particles in the aqueous dispersion and to probe the proportionality of this amount to the surface of the growing particles (A), according to

$$A = 4\pi R^2 \propto V_T^{2/3} \tag{4}$$

where R is the radius of the growing spheres and V_T the monomer volume. In Figure 5 a double-logarithmic plot of the peak area against the added monomer volume is shown for the samples discussed in Figure 3 ($T_{1.5}$).

The slope of a linear fit is determined to 0.66 for $T_{1.5}$, which is an indication that the amount of surfactant

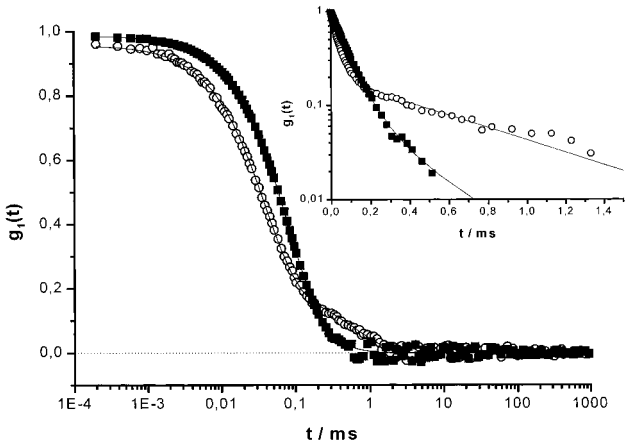

Figure 6. Field autocorrelation function $g_1(t)$ obtained for sample $T_{2.5}$ after addition of 2 g (open circles) and 25 g (filled squares) of monomer, respectively, at a scattering angle of 90°. The samples have been diluted with the AF-FFF eluent. The plot contains biexponential fits to $g_1(t)$. The inset shows the deviation for slower relaxation times more clearly.

needed to stabilize the particles is indeed proportional to their surface:

$$\log A \propto \frac{2}{3} \log V_T \tag{5}$$

From the peak area measured for the highest amount of added monomer, the amount of surfactant associated with the particles can be estimated. It is found that more than 1 g of the 1.5 g of surfactant is needed to stabilize the particles. This rough estimation supports the observation that this sample set ($T_{1.5}$), prepared using a fleet ratio of $S = 0.06$, is found to be at the edge of stability of the dispersion.

If the fleet ratio is increased to $S = 0.10$, the fractograms shown in Figure 3 are obtained for $T_{2.5}$. The particles grow homogeneously as for the sample $T_{1.5}$ (Figure 4). The resulting particles are slightly smaller as compared to $T_{1.5}$, supporting the results of Baumann et al. determined by DLS.[22] Here again, the data obtained by DLS show a significant deviation from the AF-FFF data in the range of the small particles. An example where it was possible to separate two modes of relaxation is shown in Figure 6.

The relaxation function observed for the 2 g addition clearly contains a slower mode, which is attributed to the presence of surfactant micelles due to excess surfactant.

A log−log plot for $T_{2.5}$ as shown for $T_{1.5}$ in Figure 5 yields a slope of 0.67, which is in reasonable good agreement with the theoretical value of 0.66. When comparing the peak area for the same amount of added monomer for either $T_{1.5}$ or $T_{2.5}$ and taking into account the measured radius, the number of growing particles is indeed higher for $T_{2.5}$. But since this value depends on various reaction parameters, e.g. drop rate, stirring speed, or temperature, the comparison is only qualitative.

Homogeneous DT Nanospheres. To confirm that the homogeneous growth of the particles is also found for mixtures of the chain-forming monomer dimethyldimethoxysilane (D) and the network-forming monomer methyltrimethoxysilane (T), two different sets of samples were analyzed.

In Figure 3 the AF-FFF results from the $DT30/70_{2.5}$ samples containing 30% D and 70% T (w/w) are presented.

As expected, the radius of the growing particles increases with the amount of the added monomer mixture. The homogeneous growth is confirmed by the linear dependence of the cube of the hydrodynamic radius on the added volume of the monomer mixture (Figure 4).

The slope of the linear regression for the AF-FFF data for $DT30/70_{2.5}$ is smaller as compared to the pure T nanospheres, and consequently the resulting particles are smaller. This phenomenon is interpreted by an increased number of growing particles when D is present in the monomer mixture. The DLS data of sample $DT30/70_{2.5}$ show a comparable deviation from the AF-FFF results as for $T_{2.5}$, although it was increasingly difficult to separate the relaxation of the growing nanospheres from the other structures present in the dispersion. A log−log plot of the peak area against the added monomer volume yields a slope of 0.68, confirming the proportionality between the amount of surfactant needed to stabilize the particles and their size.

The increase of the D content to 50% (w/w) yields comparable results, as demonstrated in Figure 3 ($DT50/50_{2.5}$).

A comparison of $T_{2.5}$, $DT30/70_{2.5}$, and $DT50/50_{2.5}$ shows qualitatively that the width of the distribution determined with AF-FFF increases with increasing D content. Again, the particles show homogeneous growth (Figure 4). The slope in a double-logarithmic plot of the peak area against the volume of added monomer mixture is determined to 0.66, but with a larger uncertainty. Nevertheless, this confirms also for $DT50/50_{2.5}$ that the amount of surfactant needed to stabilize the particles is proportional to their surface.

The particles become smaller with decreasing T content, from which it is concluded that the number of growing particles or nuclei increases. The number of growing particles is difficult to determine, since for example static light scattering is not suited for the determination of the molecular weight, due to the same reasons already discussed for the DLS. But when the hydrodynamic radius is compared to the corresponding peak area in the AF-FFF of the different samples, the relative number of growing particles can be calculated, assuming a comparable amount of surfactant per unit surface area. This yields factors of approximately 1.26 ($T_{2.5}$), 1.29 ($DT30/70_{2.5}$), and 2.49 ($DT50/50_{2.5}$) for the relative number of growing nuclei relative to $T_{1.5}$. This trend is also confirmed when the slopes of the relation between the cube of the hydrodynamic radius and the volume of the added monomer are compared for each sample. The slope is influenced by both the number of growing particles and their density.

The increasing content of the chain units D in the spherical particles from $T_{1.5}/T_{2.5}$ over $DT30/70_{2.5}$ to $DT50/50_{2.5}$ is also reflected in the densities of the redispersable particles, obtained in organic solvents after hydrophobization. The density decreases from $\rho = 1.38$ g/cm^3 for $T_{2.5}$ to $\rho = 1.23$ g/cm^3 for $DT30/70_{2.5}$ and to $\rho = 1.13$ for $DT50/50_{2.5}$.[23]

Core−Shell D-DT Nanospheres. The nanoparticles discussed so far exhibit a homogeneous architecture. More complex architectures may also be realized.[11,12] One example is a core−shell nanoparticle with a core composed only of the chain-forming monomer D and a

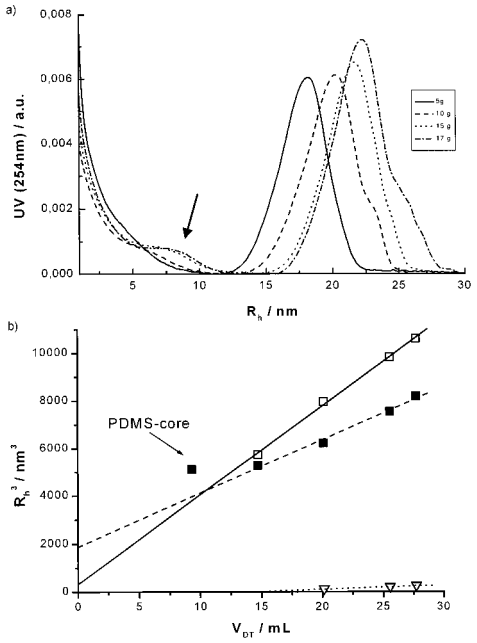

Figure 7. (a) UV signal (254 nm) of the sample D-DT30/$70_{3.0}$ obtained after addition of different amounts of monomer, as indicated by the total amount of shell-forming monomer after each addition. The samples were diluted with the eluent 1:40 (v/v). The calibration was used to translate the retention time into the corresponding hydrodynamic radius R_h. The arrow indicates the newly nucleated particles. (b) Comparison of the cube of the mean particle hydrodynamic radius obtained by AF-FFF (open squares, open triangles) and DLS (filled squares) for D-DT30/$70_{3.0}$, plotted against the added monomer volume. The arrow indicates the result observed with DLS after addition of 8 g of D.

shell composed of a mixture of 30% D and 70% T (w/w, D-DT30/$70_{3.0}$).

The chains formed in the first step have molecular weights between 1000 and 3000 g/mol.[11] Since the membrane used for the AF-FFF experiments has a molecular weight cutoff of 10 000 g/mol, these chains cannot be analyzed with AF-FFF. Only after addition of the shell forming monomers, which stabilize the particles by cross-linking, AF-FFF measurements are possible (Figure 7).

Here, a slight tendency for secondary nucleation upon addition of the monomer mixture building the shell is observed. The linear relationship between the cube of the hydrodynamic radius and the added monomer volume yields a theoretical core built of the PDMS chains of approximately 15 nm for the large particles (Figure 7b). The growth of the smaller particles is also found to be homogeneous. DLS, on the other hand, gives the weighted average size of the particles present in the dispersion. The secondary nucleation is suppressed, when less surfactant is employed in the synthesis. In this case AF-FFF delivers important constructive feedback information for the improvement of the synthesis.

Conclusion

AF-FFF proves to be a suitable tool to analyze the polyorganosiloxane nanoparticles in aqueous dispersion. The membrane, which serves as accumulation wall, ensures the removal of excess surfactant, which hinders the characterization of the particles, for instance, by dynamic light scattering. When the bifunctional monomer diethoxydimethylsilane (D) is employed together with the trifunctional monomer methyltrimethoxysilane (T), an increase in the number of growing particles is found. This effect is accompanied by the formation of smaller particles and somewhat broader distributions. From all dispersions examined, the conclusion is made that the particles show a homogeneous growth for each individual monomer addition during the polycondensation reaction in aqueous dispersion.

With AF-FFF it has been possible to identify secondary nucleation when different monomers and excess surfactant are employed and core−shell architectures are assembled. This information is now being used to optimize the synthesis for each individual monomer mixture and sequence by adjusting the amount of surfactant. To obtain information about the absolute number of growing particles, a coupling of AF-FFF with multiangle laser light scattering (MALLS)[24] seems to be the ultimate characterization procedure which will be implemented in our lab in the near future.

Acknowledgment. We thank Wacker Chemie, Burghausen, for the generous gift of monomers, Consenxus, Ober-Hilbersheim, for their uncomplicated and direct help, J. Othegraven and E. Bartsch for the PS-Latices, N. Cameron, McGill University, Montreal, Canada, for critically reading the manuscript, and the BMBF (FKZ 03C0288A8) and the Fonds der Chemischen Industrie for financial support.

References and Notes

(1) Mächtle, W. In *Analytical Ultracentrifugation in Biochemistry and Polymer Science*; Harding, S. E., Rowe, A. J., Horton, J. C., Eds.; The Royal Society: Cambridge, 1992.
(2) Schärtl, W.; Lindenblatt, G.; Strack, A.; Dziezok, P.; Schmidt, M. *Prog. Colloid Polym. Sci.* **1998**, *110*, 285.
(3) Wahlund, K.-G.; Giddings, J. C. *Anal. Chem.* **1987**, *59*, 1332.
(4) Cölfen, H.; Antonietti, M. *New Dev. Polym. Analytics* **2000**, *150*, 67.
(5) Baumann, F.; Schmidt, M.; Deubzer, B.; Geck, M.; Dauth, J. *Macromolecules* **1994**, *27*, 6102.
(6) Baumann, F.; Deubzer, B.; Geck, M.; Dauth, J.; Schmidt, M. *Macromolecules* **1997**, *30*, 7568.
(7) Baumann, F.; Deubzer, B.; Geck, M.; Dauth, J.; Sheiko, S.; Schmidt, M. *Adv. Mater.* **1997**, *12*, 955.
(8) Maskos, M.; Jungmann, N.; Schmidt, M. *Polym. Prepr.* **2001**, *42*, 90.
(9) Stöber, W.; Fink, A.; Bohn, E. *J. Colloid Interface Sci.* **1968**, *26*, 62.
(10) van Blaaderen, A.; Vrij, A. In *The Colloid Chemistry of Silica*; Bergna, H. E., Ed.; Advances in Chemistry Series 234; American Chemical Society: Washington, DC, 1994.
(11) Emmerich, O.; Hugenberg, N.; Schmidt, M.; Sheiko, S.; Baumann, F.; Deubzer, B.; Weis, J.; Ebenhoch, J. *Adv. Mater.* **1999**, *11*, 1299.
(12) Roos, C.; Schmidt, M.; Ebenhoch, J.; Baumann, F.; Deubzer, B.; Weis, J. *Adv. Mater.* **1999**, *11*, 761.
(13) Berne, B. J.; Pecora, R. *Dynamic Light Scattering*; J. Wiley: New York, 1976.
(14) Tank, C.; Antonietti, M. *Macromol. Chem. Phys.* **1996**, *197*, 2943.
(15) Wahlund, K.-G.; Giddings, J. C. *Anal. Chem.* **1989**, *59*, 1332.
(16) Wahlund, K.-G.; Litzén, A. *J. Chromatogr.* **1989**, *461*, 73.
(17) Wahlund, K.-G.; Litzén, A. *J. Chromatogr.* **1991**, *548*, 393.
(18) Litzén, A.; Wahlund, K.-G. *Anal. Chem.* **1991**, *63*, 1001.
(19) Paradies, H.; Thies, M. *Ber. Bunsen-Ges. Phys. Chem.* **1994**, *98*, 715.
(20) Paradies, H.; Hinze, U.; Thies, M. *Ber. Bunsen-Ges. Phys. Chem.* **1994**, *98*, 938.
(21) Emmerich, O. Ph.D. Thesis, University of Mainz, Germany, 1999.
(22) Baumann, F. Ph.D. Thesis, University of Bayreuth, Germany, 1995.
(23) Graf, C.; Schärtl, W.; Maskos, M.; Schmidt, M. *J. Chem. Phys.* **2000**, *112*, 3031. Jungmann, N. Ph.D. Thesis, University of Mainz, Germany, 2000 (http://archimed.uni-mainz.de/).
(24) White, R. J. *Polym. Int.* **1997**, *43*, 373.

MA0106752